Physicochemical Characterization of Biomass Residue–Derived Biochars in Vietnam

Nguyen Van Hien[a,b], Eugenia Valsami-Jones[a], Nguyen Cong Vinh[b] , Tong Thi Phu[b], Nguyen Thi Thanh Tam[b], Iseult Lynch[a*]

[a] School of Geography, Earth and Environmental Sciences, University of Birmingham, Edgbaston, B15 2TT, UK

[b] Department of Land Use, Soils and Fertilizers Research Institute, Hanoi, Vietnam

[*] Corresponding author: i.lynch@bham.ac.uk

Abstract

This study compares the physico-chemical characteristics of three different types of biochar produced from biomass residues in Vietnam as a basis for optimising their application in water purification and soil fertilisation. Wood biochar (WBC), rice husk biochar (RBC), and bamboo biochar (BBC) were produced under limited oxygen conditions using equipment available locally in Vietnam, known as a Top-Lid Updraft Drum (TLUD). The resulting biochars were characterised using a suite of state-of-the-art methods to understand their morphology, surface chemistry and cation exchange capacity. Surface areas (measured by BET) for WBC and BBC were 479.34 m^2/g and 434.53 m^2/g, respectively, significantly higher than that of RBC which was only 3.29 m^2/g. The morphology as shown in SEM images corresponds with the BET surface area, showing a smooth surface for RBC, a hollow surface for BBC, and a rough surface for WBC. All three biochars produced alkaline, with pH values around 10, and all have high carbon contents (47.95 - 82.1 %). Cation exchange capacity (CEC) was significantly different ($p<0.05$) among the biochars, being 26.70 cmol/kg for RBC, 20.7 cmol/kg for BBC, and 13.53 cmol/kg for WBC, which relates to the cations (Ca, Mg, K) and functional groups with negative charge (carboxyl, hydroxyl) present on the biochar surfaces. The highest contents of Ca, Mg and K in rice husk BC may explain its highest CEC values. Thus, although the biochars were produced by the same method, the various feedstocks lead to quite different physico-chemical properties. Ongoing work is linking these physico-chemical properties to the biochar efficiencies in terms of nitrate and ammonia capture capacities for use as fertilisers, and for adsorption of heavy metals (Zn, Cu) or water filtration, in order to design optimal biochar properties for specific applications.

Key words: physico-chemical characteristics, biochar, BET surface area, SEM, total carbon, CEC, FTIR, feedstock

Preprints (www.preprints.org) | NOT PEER-REVIEWED | Posted: 22 July 2018 doi:10.20944/preprints201807.0403.v1

1. Introduction

Biochar is the carbonized product gained by pyrolysis of biomass under restricted or absent oxygen conditions,[1] but without an activation step and thus differs from so-called activated carbon.[2] The justification for carbonization through pyrolysis is to avoid the negative influences on human health and the environment that result from direct (in field) burning of biomass residues which releases carbon dioxide, one of the most important greenhouse gases.[3] Biomass-derived biochar is formed via a complex process,[4] but the reaction mechanism of biomass pyrolysis can be described as occurring mainly via three steps,[5] as follows:

$$\text{Stage 1: Biomass} \xrightarrow{\text{Heat}} \text{Moisture + Dry residues}$$

$$\text{Stage 2: Dry residues} \xrightarrow{\text{Heat}} \text{(Volatile and Gases) + Pre-biochar}$$

$$\text{Stage 3: Pre-biochar} \xrightarrow{\text{Heat}} \text{(Volatile and Gases) + Biochar}$$

The first step is loss of moisture from the biomass, which becomes dry feedstock by heating. Then pre-biochar and volatile compounds are formed. In the last step, chemical compounds in the biosolid rearrange and form a carbon-rich solid product known as biochar. The volatiles, are either condensable such as bio-oil, or noncondensable gases[6] known as syngas, including hydrogen (50%), carbon dioxides (30%), nitrogen (5%), methane (5%), and others[7]. As a result of its aromatic structure,[8] biochar can be recalcitrant to microbial decomposition and mineralization,[9] which leads to its persistence in soil for hundreds of years.[9] In fact, biochar found in dark soil known as 'Terra Preta soil' in Amazônia was reported as being about 500-2,500 years old,[10] while biochar found in ocean sediment was estimated to date from 2,400 to 13,000 years ago [11].

The benefits of biochar were demonstrated by several previous research efforts. For instance, wood biochar applied into a Colombian savanna Oxisol increased available Ca and Mg concentrations and pH, and reduced toxicity of Al.[12] In addition, biochar improved soil structure,[13] created a carbon sink in soil,[14] and reduced CH_4 emissions.[15] Hale et al.[16] reported that biochar can absorb NH_4^+-N via cation exchange, thereby reducing the leaching of nitrogen fertilizer from soil.[17] Interestingly, biochar can be recalcitrant to microbial attack,[18] while compost or plant

biomass are rapidly decomposed to greenhouse gases (CH_4, CO_2), especially in tropical regions.[19] Thus, the application of biochar has a positive effect on soil fertility, particularly in tropical regions.[20] However, several studies have found no or negative influences of biochar application. For example, in calcareous soils, biochar did not improve pH or available P and cations.[21] Additionally, greenhouse gas emission (CO_2) was increased for an Inceptisol type soil to which wood biochar produced at 350°C was applied.[22] These disadvantages may relate to biomass type and conditions of biochar production, and soil type.

Pyrolysis conditions impact on the physicochemical characteristics of the biochar.[23] For example, Méndez, et al. [24] observed that the ash content, pH, and BET surface area increased, while CEC, volatile matter and microspore area declined in biochar produced from sewage sludge at 600 °C compared to biochar prepared at 400 °C. On the other hand, a dramatic increase from 0.007 m^2/g to 274 m^2/g in micropore (defined as being < 2 nm) area was observed for biochars derived from Cottonseed hull when the pyrolysis temperature increased from 650 °C to 800 °C.[25] Decreases in total N, organic carbon (OC), and CEC were also found in poultry litter biochar when the pyrolysis temperature rose from 300 °C to 600 °C, while the opposite trend was seen for pH and BET surface area.[26] Similar trends also were observed by Mukherjee et al. [27] and Chen, et al. [28] who explained that at low temperature (<300 °C) compounds containing -OH, aliphatic C-O and ester C=O groups were removed from the outer surface, while volatile matter shielding or connecting to aromatic cores were destroyed or partly emitted at higher temperatures (>300 °C). Thus, micropores dominating the biochar surface are filled by volatile compounds, which are emitted during pyrolysis as the temperature increases [27] and dramatically enlarge the surface area of the resulting biochar.[29]

The biomass materials used for biochar production also have a major influence on the resulting biochar properties.[30] For instance, wood and grass biomass-derived biochar normally contain low nutrient elements, in part due to emissions of nitrogen during the pyrolysis process, so the resulting biochar has much lower N content than fertilizers.[31] Song and Guo [26] reported that biochars formed from waste wheat straw and tree leaves contained higher organic carbon (OC) content (64% - 73.9%) than that of poultry litter-derived biochar (36.10%) produced at the same temperature (400 °C). In addition, the different original biomass affects the morphology of the resulting biochar; for instance, the exoskeleton of tracheids (elongated cells in the xylem of

Preprints (www.preprints.org) | NOT PEER-REVIEWED | Posted: 22 July 2018 doi:10.20944/preprints201807.0403.v1

vascular plants that serve in the transport of water and mineral salts) was an important contributor to structure for wood biochar, while a heterogeneous structure resulted from chicken manure biochar.[32] The CEC and pH of poultry litter-produced biochar were observed to be higher than those of pine chip biochar and peanut hull biochar.[33]

The properties of biochar are not static once formed: the environmental conditions following biochar application were also found to affect biochar properties.[34] Surface oxidation of biochar particles was observed to occur when the biochar was applied into soil,[35] resulting in an increase of between 10% and 16% in surface negative charge (carboxyl groups) of biochars (350-600 ^{o}C) derived from corn stover residues and oak wood when applied under alternative water regimes (i.e. wet and dry conditions).[34] However, aliphatic groups (CH_2, CH_3) were decreased by 18-42% in the wet conditions, and by 4-30% in the dry conditions.[34] Cheng, et al. [36] reported that abiotic oxidation governed the increase of negative surface charge and CEC of wood biochar (black locust) in soil, rather than biotic oxidation (microbial activities). Surface oxidation increased over time, progressing from phenolic groups to carboxylic groups, which were the main (cation) adsorption sites of the biochar.[36] Yang, et al. [37] reported that the content of C=O and COOH groups of walnut shell biochar incubated with $FeCl_3$ or kaolinite was enhanced 2.0 and 2.5 times, respectively, compared with the fresh biochar. The surface groups of the fresh biochars were negatively charged and so adsorbed only cations (NH_4^+) via CEC.[27] However, the O-containing groups of biochar could react with soil cations such as Al^{3+}, Fe^{3+}/Fe^{2+}, Ca^{2+}, Mg^{2+} to form organometallic complexes,[37] and therefore could adsorb nutrient anions such as NO_3^-, PO_4^{3-}.[27]

Biochar application has thus been shown to have positive effects on the physico-chemical properties of soil. However, as different biomass and pyrolysis conditions give various biochar characteristics, which have different effects on soil properties and plants, it is not always clear what the optimal biomass composition should be for specific local applications. Vietnam, for example, has tropical weather leading to highly decomposed soil organic matter, and has high rain annual fall causing severe erosion and leaching. Currently, the agricultural and forestry residues in several regions in Vietnam are burnt or left to decompose in the fields, which results in carbon dioxide release from the biomass into the atmosphere. Therefore, turning the biomass into biochar will bring more benefits for soil enrichment and reduce the environmental impact of agriculture. Hence, the objectives of this study were to identify the physicochemical properties of

three different biochars formed from acacia wood chip, rice husk, and bamboo by the Top-Lid Updraft Drum (TLUD) technology, a biomass production method commonly used in this region.

2. Materials and methods

2.1. Biochar production

•Materials for biochar production:

The biomass residues used for biochar production in this study were collected from small processing factories in a suburb of Hanoi city. The feedstocks include acacia wood chip, rice husk and bamboo. The wood and bamboo were chopped into suitable pieces to fit into the Top-Lid Updraft Drum equipment and air-dried before the pyrolysis process. According to Nasser and Aref [38] the chemical composition of acacia wood is 48% of cellulose, 22% hemicelluloses, and 30% lignin, while rice husk contains 28-38% cellulose, 9-20% lignin, and 18.8-22.3% SiO_2.[39] In comparison, bamboo is 47.5% cellulose, 15.35% hemicelluloses, 26.25% lignin, and 0.7% silica.[40]

•Technology of biochar production

The TLUD technology was inherited from the project 'Piloting Pyrolytic Cookstoves and Sustainable Biochar Soil Enrichment in Northern Vietnam Uplands' (Grant Agreement No 3-V-048). It consisted of a barrel (55 gallon, height 34.5 inch, diameter 23 inch) with a chimney, which is described in detail in Figure 1. The three different biochars were produced simultaneously in a TLUD that has been modified to allow the use of various feedstocks in parallel, resulting in biochars produced under identical conditions. The materials are put into the drum in parallel layers of about 20 cm thickness to ensure uniformity in temperature for each feedstock. The final layer is wood, as wood keeps the flame for a long time, and thus is used to reduce the smoke formed during the pyrolysis process. A fire is started at the top of the material and then the lid and chimney are placed on top, once a flame is established. After the biochar starts to form, small amounts of water are injected inside the drum via the 16 hole (d = 5 cm) and 8 hole (d = 5 cm) rows in order to maintain a temperature between 400 – 550 ^{o}C. The total process takes about 3 hours, then the lid is removed and water is sprayed inside the drum to extinguish the fire and cool the biochar. Upon cooling, the layers of biochar can be removed and separated. After that, 1kg of each biochar from wood (WBC), rice husk (RBC), and bamboo (BBC) biomass was stored in air tight plastic bags and shipped to the University of Birmingham, UK. Finally, the samples were kept at room temperature in the lab for analysis. The samples were characterized

Preprints (www.preprints.org) | NOT PEER-REVIEWED | Posted: 22 July 2018 doi:10.20944/preprints201807.0403.v1

through BET surface area, Scanning Electron Microscopy (SEM), Fourier transform infrared spectroscopy (FTIR), elemental and proximate analysis, and CEC, with reference to the COST Action guidelines for standardisation of biochar analysis[41] where appropriate.

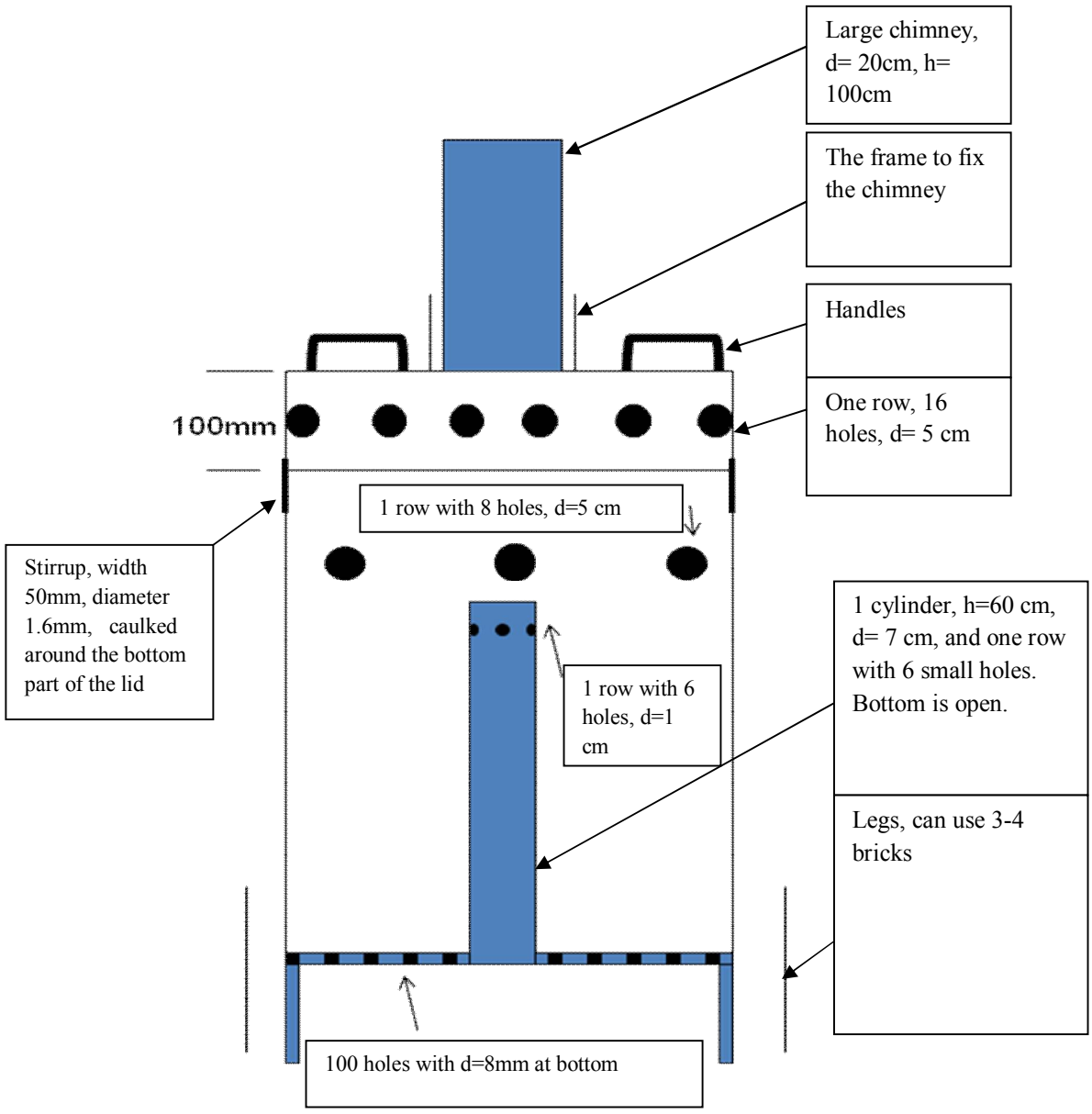

Figure 1: Modified TLUD for biochar production

2.2. Analysis methods

pH_{H2O} analysis:

Biochars, sieved through a 2mm mesh, were analyzed for pH using the method of [42]. Briefly, distilled water, with ratio of biochar to DI water of 1:25 (w/v), was added to the biochar and the mixture was shaken for 1.5h to ensure good contact between the water and the biochar's internal

Preprints (www.preprints.org) | NOT PEER-REVIEWED | Posted: 22 July 2018 doi:10.20944/preprints201807.0403.v1

surface. Then, the solvent was stirred again by steel spatula and pH of the solvent was continuously measured using a Thermo Orion 3 star pH meter.

Cation exchange capacity (CEC):

CEC was determined using the method described in [42]. In brief, 1.0 g of the biochar sieved through a 2mm mesh was saturated with 50 mL of 1N CH_3COONH_4 (pH=7) and the mixture solution was shaken on a shaker table overnight which ensured that the biochar surfaces were sufficiently wetted. After shaking, the solution was filtered by vacuum filter (0.22 µm) and then an additional 40 mL of the 1N CH_3COONH_4 was added and then immediately extracted by the filtration. Next, 60 ml of ethanol (80%) was used to wash all unbound NH_4^+ from around the samples. The biochar samples were placed into a glass beaker and 50 mL of 1N KCl was added. The solution was kept for 16 h in order to reach equilibrium during which time the NH_4^+ absorbed to the biochar was completely replaced by K^+, then immediately another 40 mL of 1N KCl was added for a subsequent extraction. The solutions containing NH_4^+ which replaced by K^+ were quantified by Ion Chromatography (Dionex DX500) using 6 standards (0, 0.5, 1.0, 5.0, 10.0, 20, 50 mg/L of NH_4^+).

Scanning electron microscopy (SEM):

Small pieces of initial biochar were selected and further dried at 60 ^oC in an oven overnight. Then, 4-5 small pieces of each biochar sample were coated with 10 nm Au/Pt film by a Cressington SC7640 sputter coater and kept in a desiccator overnight. A scanning electron microscope (Philips ESEM XL30 FEG model) operating at accelerating voltages of 10-20 kV was used to image the biochars.

BET surface area:

Surface area was determined by the Brunauer, Emmett, and Teller (BET) method (1983). The method is based on Langmuir's theory for monolayer molecular adsorption to multilayer adsorption with the hypotheses that physical adsorption of gas molecules onto a solid occurs in layers, with no interaction between each adsorption layer. A Surface Area Analyzer (model SA 3100) was used for this analysis. Approximately 1g of biochar (adsorbent), sieved through a 2mm mesh, was loaded into the vessel. Prior to the determination of the adsorption isotherm, outgassing was conducted to remove the physically adsorbed substances from the adsorbent at

Preprints (www.preprints.org) | NOT PEER-REVIEWED | Posted: 22 July 2018 doi:10.20944/preprints201807.0403.v1

250 °C for three hours. After degassing was complete, the sample vessel was weighed to determine exactly the weight of the adsorbent, which was used for BET surface analysis. Then, a known volume of nitrogen gas (adsorbate) was admitted into the sample vessel at cryogenic temperature by the gas adsorption technique. The pressure in the sample vessels was measured for each volume of the gas added until the adsorbate and adsorbent are in equilibrium. The surface area of the samples was measured by plotting the data as straight line with y= 1/v[(P/Po)-1] and x=P/Po following equations (equations 1 and 2):[43]

$$\frac{1}{V\left[\left(\frac{P_0}{P}\right)-1\right]} = \frac{C-1}{C}\left(\frac{P}{P_0}\right) + \frac{1}{V_m C} \qquad \text{(equation 1)}$$

where P_0 and P are the equilibrium and the saturation pressure of the adsorbate, V is the volume of adsorbed gas, and V_m is the volume of the monolayer-adsorbed gas, C is BET constant, and:

$$C = \exp\left(\frac{E_1 - E_l}{RT}\right) \qquad \text{(equation 2)}$$

where E_1 and E_l are the heats of adsorption for the first and higher layers, respectively.

A total surface area $S_{BET,total}$ and a specific surface area S_{BET} were estimated using the following equation (equation 3):

$$S_{BET,total} = \frac{V_m N s}{V} \quad \text{and} \quad S_{BET} = \frac{S_{total}}{\alpha} \qquad \text{(equation 3)}$$

where N is Avogadro's number, s is the adsorption cross section of the adsorbing species, α is the mass of adsorbent (g).

Proximate analysis:

Moisture, ash, and volatile matter were analysed by the method of the American Society for Testing and Materials Standard (ASTM standard –D1762-84). Approximately 1g of biochar, sieved through a 2mm mesh, was added into a porcelain crucible and the moisture content was calculated from the loss in weight at 105 °C in the oven for 2h. After that, the crucibles used for moisture measurement were heated to 950 °C in a muffle furnace for a period of 6 minutes to measure volatile mater. Ash content was then calculated from the loss in weight of the samples contained in the crucibles (used for volatile matter) following heating at 750 °C for 6h.

Preprints (www.preprints.org) | NOT PEER-REVIEWED | Posted: 22 July 2018 doi:10.20944/preprints201807.0403.v1

Elemental analysis (C, N, H):

5mg of biochar, sieved through a 2mm mesh, was loaded into a tin capsule and placed into an autosampler drum to remove any atmospheric nitrogen. The sample was then put into a vertical quartz tube and heated at 1,000 ^{o}C with constant helium flow and pure oxygen in order to combust (oxidize) the sample completely. The gas mixture containing the three components (C, N, H) from the oxidation step was separated via a chromatographic column and detected by a thermoconductivity detector. The elemental analyzer used was a Carlo Erba EA1110 Model, Italy. The total O was calculated following the ASTM method as follows:

$$O\ (\%w/w) = 100 - ash\ (\%w/w) - C\ (\%w/w) - N\ (\%w/w) - H\ (\%w/w) \quad \text{(equation 4)}.$$

Total P, Ca, Mg, and K:

Total P, Ca, Mg, K were measured after biochar (0.5g) was put into a porcelain crucible heated to 500°C over 2 h, and held at 500 °C for 8 h for dry combustion. The sample was then moved into the combustion vessel. Next, 5 mL HNO_3 was added to each vessel and the samples were digested by a heating block at 120°C until dryness (5h). The tubes were allowed to cool before adding 1.0 mL HNO_3 and 4.0 mL H_2O_2. After that, samples were preheated to 120°C to dryness, and then dissolved with 1.43 mL HNO_3, made up with 18.57 mL deionized water to achieve 5% acid concentration, sonicated for 10 min, and filtered. The total P was measured by spectroscopy using a UV-Vis 2000 model with quartz cuvette at λ=725 nm with 6 standards (0, 0.02, 0.04, 0.06, 0.08, 0.1 mg P_2O_5/100mL) to establish the standard curve. Ca and Mg were titrated by EDTA (0.01 M) with murexide (the ammonium salt of purpuric acid) indicator for Ca and Eriochrome Black T for Mg, and K was analyzed by Flame Atomic Adsorption Spectroscopy (FAAS 2900 model) with 4 standards (0.25, 0.5, 1.0, and 2.0 mg K/L).

Fourier-transform infrared (FTIR) spectroscopy:

Approximately 0.5 g of biochar, sieved through a 2mm mesh and dried at 60^{o}C, was used for FTIR analysis. The FTIR spectra of the biochar were measured using a Varian 660 spectrometer. The spectra were an average of 32 scans at 4 cm^{-1} resolution from 4000–400 cm^{-1} region.

Statistical analysis:

Microsoft office excel 2007 was used for determination of standard deviation (SD) and T-test: Two-Sample Assuming Unequal Variances.

Preprints (www.preprints.org) | NOT PEER-REVIEWED | Posted: 22 July 2018 doi:10.20944/preprints201807.0403.v1

3. Results and discussion

3.1. Elemental components

The biochar samples were analyzed in duplicate for C, H, N, P, K, Ca, and Mg, whereas O was calculated using equation 4 shown in section 2.2 above. The data are presented as mean ± SD (standard deviation) in Table 1. Results indicate that all three biochars had high carbon content, and that there was a difference ($p<0.05$) among the biochars. Wood BC had the highest value (82.10 ± 0.21 %C), while rice husk BC was lowest with only 47.82 ± 0.18 %C. A high carbon concentration is an important property of biochar for soil enrichment. Nitrogen (N) accounted for a very low proportion in the ultimate analysis, with similar values ($p>0.05$) for all three biochar samples with N in the range 0.62 ± 0.06 - 0.72 ± 0.02% N in the order rice husk BC < wood BC < bamboo BC. Hydrogen content was also low and similar across the three biochars, ranging from 2.07 ± 0.04) % to 2.33 (± 0.01%) H, with wood BC < rice husk BC = bamboo BC. Unlike the carbon content, the oxygen content of rice husk and bamboo were similar ($p>0.05$), fluctuating between 8.25 ± 0.28% and 8.86 ± 0.02%, whereas wood biochar oxygen was 12.93 ± 0.16%. There was no statistical difference of phosphorous (P_2O_5) content ($p>0.05$) among the biochars nor for potassium (K) or magnesium (Mg), although the absolute values varied. However, the Ca content of rice husk BC (2.37 ± 0.18 %) was significantly different ($p<0.05$) in comparison with those of wood BC (0.65 ± 0.06%) and bamboo BC (0.57 ± 0.01%).

Table 1. Elemental composition of the three different biochar samples

Parameters	Wood BC	Rice husk BC	Bamboo BC
C, %	82.10 ±0.21	47.82 ±0.18	80.27 ±0.08
H, %	2.33 ±0.01	2.07 ±0.04	2.07 ±0.04
N, %	0.71 ±0.05	0.62 ±0.06	0.72 ±0.02
O, %	12.93 ±0.16	8.25 ±0.28	8.86 ±0.02
P_2O_5,%	0.51 ±0.21	0.50 ±0.20	0.19 ±0.13
K,%	1.58 ±0.62	1.89 ±0.63	0.47 ±0.13
Ca,%	0.65 ±0.06	2.37 ±0.18	0.57 ±0.01
Mg,%	0.21 ±0.05	0.26 ±0.10	0.14 ±0.03

The biochars produced from plant residues normally contain a low portion of nutrient elements.[31] The loss of H and N via volatile matter is related to the degree of carbonization during pyrolysis, explaining in part the low H and N values.[44] Cantrell *et al.* reported that H and N contents in initial biomass were volatised 50-85% and 21.4%-77.5%, respectively, when pyrolysis temperatures increased from 350 °C to 700 °C.[31] However, N content can be preserved in biochar due to the transformation of the amine functionality in the original feedstocks into pyridine-like compounds during pyrolysis.[44] The very low N contents determined here (Table 1) suggests that most were volatilised, and that low pyridine functionality can be expected from the FTIR analysis.

3.2. Proximate analysis, pH and CEC of the biochar samples

Samples were run in duplicate for moisture, volatile mater, and ash proportions, and in triplicate for pH and CEC. The results are shown in Table 2 and are presented as mean ± SD. The data indicate that the biochars were all alkaline with pH values ranging from 9.51 (± 0.02) to 10.11 (± 0.04) in the order Rice BC < Bamboo BC < Wood BC. Several previous studies proved that the alkalinity of biochar is attributed to the presence of alkaline metals such as Ca, Mg, and K,[26, 45] carbonate ($CaCO_3$ and $MgCO_3$), and organic functional groups.[46] This is consistent with the data from Table 1, where the Rice husk BC had the highest values of Ca, Mg and K, and the Bamboo BC having the lowest concentrations of each. The pH is known as a pivotal parameter of soils, which impacts on available nutrients and plant growth.[47] Thus, the high pH of these biochars suggests their suitability for use as soil amendments to ameliorate acidic soils,[47] which may also contain aluminium, iron and manganese which can be toxic to crops and cause nutrient (P, Mo, Mg, Ca) deficiencies in several soils.[46] For example, Fe^{2+} is toxic to rice when soil pH<5.0 due to excessive Fe^{2+} uptake. A high Fe^{2+} content in soil can also lead to poor root oxidation due to accumulation in the rhizosphere of H_2S and FeS which inhibit respiration.[46]

The ash content of the biochars, as determined by the ASTM method, shows significant differences among the various biochars ($p<0.05$). The largest proportion of ash was found in the rice husk BC, with 41.24 (± 0.49) % ash, while the lowest was observed for wood BC (1.93 ± 0.03 %). Rice husk BC has been reported previously to have a relatively high ash content, e.g., 54.0% [48] which is due to the biomass having lower abundance of lignin, e.g., 9-20% [39] as compared to woody residues, e.g., 20-40%.[49] In addition, biochar with higher ash contents was found to correspond to lower values of fixed carbon, as reported in several previous studies.e.g.[50]

Preprints (www.preprints.org) | NOT PEER-REVIEWED | Posted: 22 July 2018 doi:10.20944/preprints201807.0403.v1

Interestingly, although there were significant differences ($p<0.05$) in both the ash and fixed carbon (rice husk BC < bamboo BC < wood BC) proportions among the biochars, their volatile matter values were similar ($p>0.05$), ranging between 45.61 (± 0.54) % and 48.72 (± 3.22) % (rice husk BC < wood BC < bamboo BC). The low fixed carbon content of rice husk BC (7.82 ± 0.10 %) means that this material is less resistant to biotic decomposition and thus has a shorter existence in soil.[50a] However, rice husk BC's high pH and CEC are useful properties for soil enrichment.[51]

Table 2. CEC, pH, and composition of the three biochars

Parameters	Wood BC	Rice husk BC	Bamboo BC
pH	10.11 ±0.04	9.51 ±0.02	9.94 ±0.02
CEC, Cmol/kg	13.53 ±0.65	26.70 ±1.57	20.77 ±1.21
Moisture,%	5.45 ±0.03	5.37 ±0.05	6.11 ±0.11
Volatile,%	46.68 ±1.68	45.61 ±0.54	48.72 ±3.22
Ash,%	1.93 ±0.03	41.24 ±0.49	8.08 ±0.20
Fixed carbon,%	45.94 ±1.68	7.82 ±0.10	37.09 ±3.32

There were significant differences of CEC values among the three biochars ($p<0.05$). In fact, rice husk BC had the highest CEC with 26.70 Cmol/kg, while bamboo and wood BC were 20.77 Cmol/kg and 13.53 Cmol/kg, respectively. A high CEC indicates the ability of biochar to adsorb cationic nutrients (e.g. Ca^{2+}, Mg^{2+}, NH_4^+, K^+) and thus high CEC biochars reduce the leaching of these nutrients along a soil profile.[26] CEC depends on the presence of negatively charged surface functional groups [52] and other sources like metal hydroxides and silica phytoliths in biochar ash.[53] In addition, ageing and oxidization of biochar surface following application in the environment (soil) contributes to increased CEC values,[36] thus enhancing the adsorption and retention capacities of soil for nutrient cations.[46]

3.3. FTIR spectroscopy

FTIR spectra of wood, rice husk, and bamboo BCs are shown in Figure 2. The characteristic vibration was interpreted based on Stuart [54] and Özçimen and Ersoy-Meriçboyu.[50] The band at

2922 cm^{-1} of both bamboo and wood BC refers to the aliphatic C-H stretching of alkenes. The O-H stretching of carboxylic acids in the three BCs is observed in the region of 2588-2532 cm^{-1}, while O–H and P–H stretching of ester compounds are assigned in the range of 2362-2348 cm^{-1}. The bands that appear at around 2160 cm^{-1} in rice husk and wood BC are attributed to aliphatic isonitrile –N≡C stretching, C=C stretching of alkynes, as well as Si-H stretching of silicon compounds.

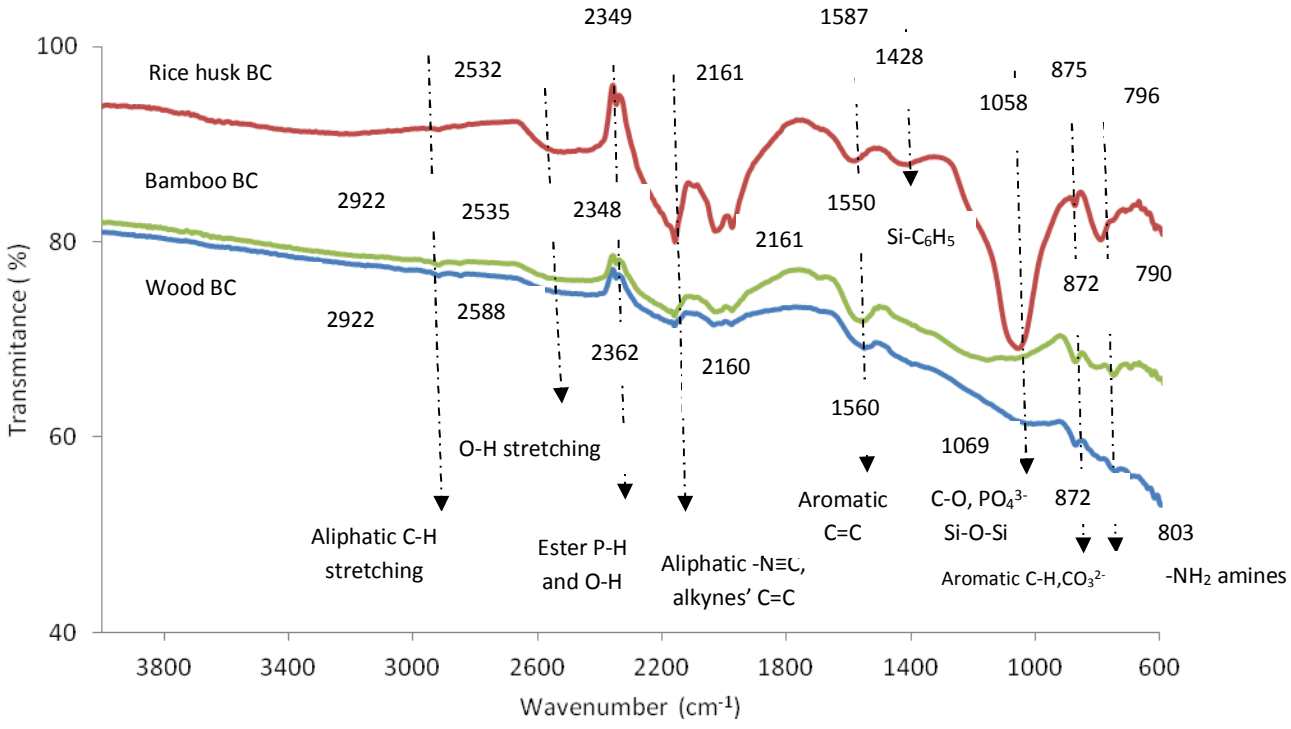

Figure 2. FTIR spectra of the three different biochars in the range 4000 – 400 cm^{-1}.

The C=C stretching bands of aromatic compounds of the biochars appeared in the range 1587-1550 cm^{-1}, whereas aromatic C=C stretching and C-H bending bands are assigned between 875 cm^{-1} and 872 cm^{-1}. Interestingly, there was one band near 1430 cm^{-1} for rice husk BC only, suggesting silicon attachment to the ring of benzene. Bands in the range of Si-O-Si asymmetric stretching (1000-1130 cm^{-1}) were observed for both wood BC (1069 cm^{-1}) and rice husk BC (1058 cm^{-1}). This finding was in contrast with the report of Nasser and Aref [38] who found no Si content in wood BC from six Acacia species in Saudi Arabia. In addition, CO_3^{2-} groups were also represented in the bands at 872 cm^{-1} for wood BC and bamboo BC or at 875 cm^{-1} for rice husk BC, while the bands appearing in the range of 950-1100 m^{-1} for wood BC (1069 m^{-1}) and rice husk BC (1058 m^{-1}) are assigned to PO_4^{3-} ions. In the range 1069-1058 cm^{-1}, C-O stretching bands of

alcohols and phenols and aliphatic C-O stretching of esters were found in wood and rice husk BC, but were not present in bamboo BC. The bands observed between 803-796 cm^{-1} for all three biochars were associated with NH_2 wagging and twisting of amines, and aliphatic symmetric P–O–C stretching. Similarly, =C-H bending of alkynes and C-S stretching bands were assigned in the range of 700-600 cm^{-1} and were present in all three biochars. Thus, the three biochars were dominated by the aromatic structure [55] which results from the transformation of cellulose, hemicelluloses, and lignin and protein present in the parental feedstocks [31, 56] to form condensed structures via aromatization [53] during the pyrolysis process. This is consistent with the alkaline pHs found for all three biochars. Additionally, carboxylic acid, alcohol, phenol, and amine functional groups were found to have formed on the biochar surfaces, which play an important role in cation and anion adsorption capacity of biochar, and indeed is consistent with the original biomass components.

3.4. BET and SEM

The BET surface area of the three biochars is presented in Figure 3, with values varying significantly with different parental biomass ($p<0.05$). The bichar produced from rice husk has the lowest BET surface area of 3.29 ± 0.02 m^2/g while bamboo and wood biochar both resulted in higher values of 434.53 ± 2.79 and 479.34 ± 0.88 m^2/g, respectively. The low value of surface area of rice husk BC corresponds with its less complicated morphology as indicated in the SEM images (Figure 4 c & d), compared to wood and bamboo BCs (Figure 4). In genaral, the surface area of biomass biochar is increased by the development of a porous system during the pyrolysis process.[1b] However, the high ash content of rice husk (41.24%, see Table 2) can result in blocking of the pores [50a] which contributes to the reduction in surface area. In addition, softening, melting, fusing, and carbonizing during pyrolysis process, which can result in significant blocking of the pores, also causes a decease of the surface area values.[57] According to Rouquerol, et al. [58] biochar porosity was characterized by the International Union of Pure and Applied Chemistry (IUPAC) as micropores (<2 nm), mesopores (2-50 nm), and macropores (>50 nm). In fact macropores do not contribute to the measured surface area, while meso- and micropores do.[47]

Scanning electron microscopy (SEM) was used to characterize the morphology of the three biochar samples. The pore shape, size and morphology are visualised by SEM, providing information on the structure of the three biochars after pyrolysis of the different biomasses.

Preprints (www.preprints.org) | NOT PEER-REVIEWED | Posted: 22 July 2018 doi:10.20944/preprints201807.0403.v1

Figure 4 shows representative images of each biochar, at two different magnifications (20 µm x 1000 µm and 200 µm x 100 µm). These pictures demonstrate the difference in porous structure among the biochars. In fact, the surface of the wood biochar has a complicated and rough surface with hollow structure (Figure 4a) and various pores (Figure 4b), representative of volatile compound release.[59] In contrast, the morphology of rice husk shows elongated hollow regions (resembling the shape of a boat) (Figure 4d) with one side having rough surface formed by mostly closed vesicles in rows, which were presumably formed by the melting of lignin while transporting the volatiles towards the surface [60] and cracking and polymerization of hydrocarbons.[61] In addition, there are crystals of inorganic salts present as individual particles and soot particles [61] covering the surface (figure 4c). In contrast, the other side of the wood biochar (Figure 4d) was observed as a smooth surface. Liu, et al. [62] reported that the melting and fusion process of lignin and other small organic molecules could be the cause of smooth surface formation.

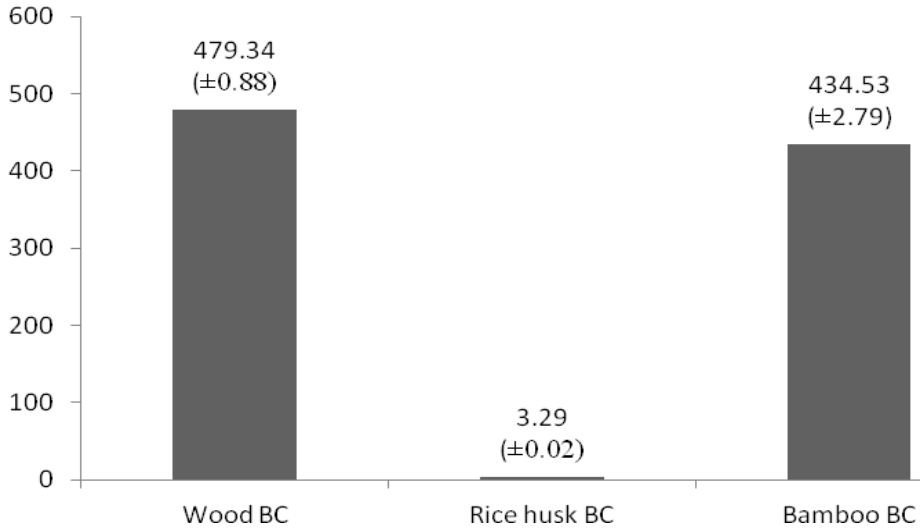

Figure 3. BET surface area of three different biochars.

Several mineral crystals (Figure 4a) were observed on the surface of rice husk BC. Septien, et al. [63] proposed that the mineral grains moved to the surface and then coalesced after fusion or re-condensed volatiles. Interestingly, the porous structure did not show on the SEM images of rice husk BC, while this parameter plays a key role in surface area of biochar, particularly, mesopores and micropores.[47] In addition, a porous system serves as habitat for soil microorganisms such as bacteria, fungi, and protozoa which interact with the rhizophere to improve the ability of plant for nutrient uptake.[64] Thus, these limitations suggest that risk husk BC may be less suitable as a soil

Preprints (www.preprints.org) | NOT PEER-REVIEWED | Posted: 22 July 2018 doi:10.20944/preprints201807.0403.v1

nutrient, due to the lower BET surface area of this biochar. In comparison, bamboo BC (Figure 4e & f) had a special morphology, appearing as a hollow honeycomb-like structure with various pore sizes. The volatile compounds released quickly during the pyrolysis process created an internal overpressure and led to the coalescence of small pores, which lead to inner cavities and a more open structure.[65] Such open pores with dominant micropores are the main source of this biochar's high surface area [60]. Thus, the complicated surface structure of both wood BC and bamboo BC allows them to have higher BET surfaces than rice husk BC.

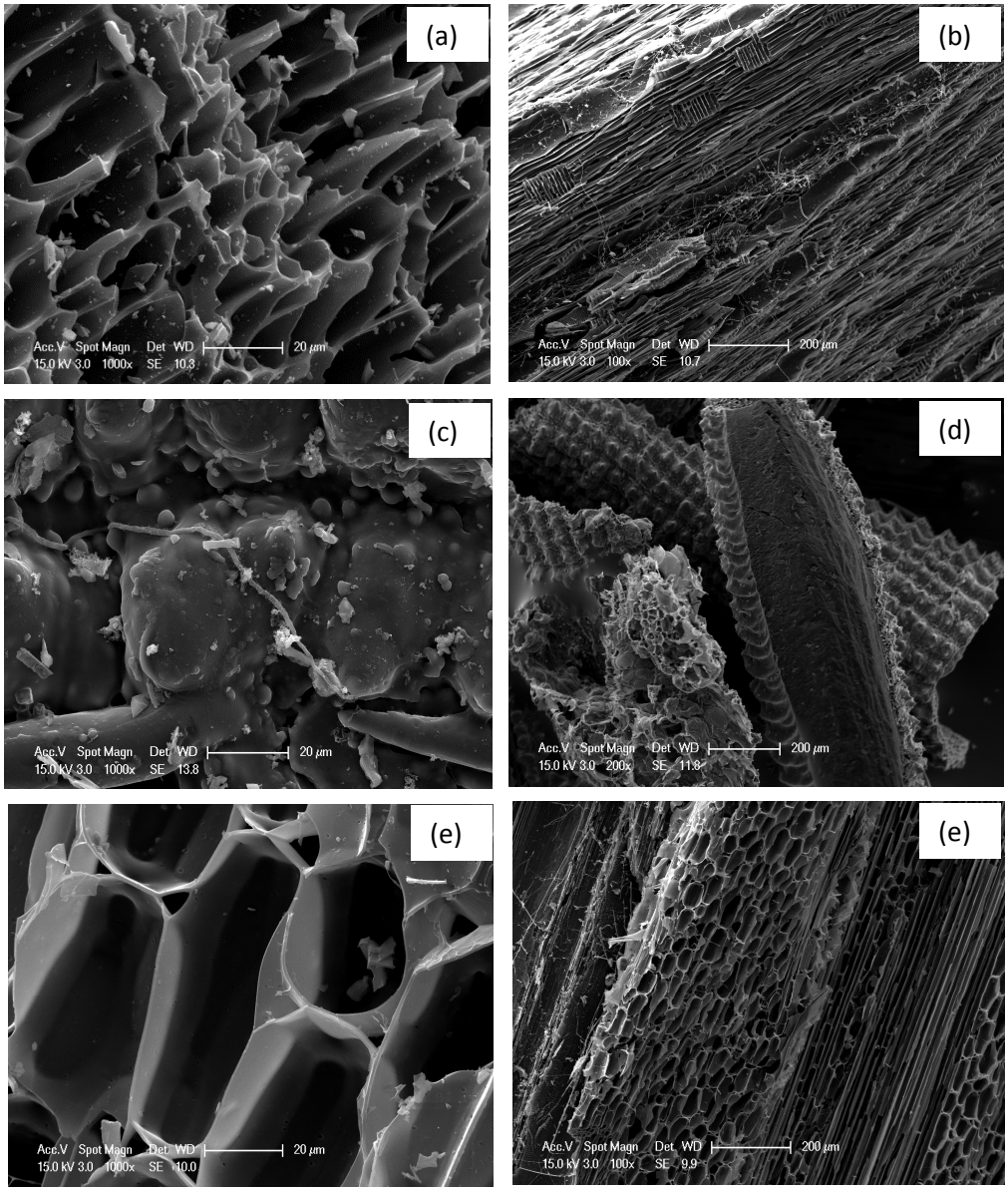

Figure 4. SEM photographs of biochar samples, (a, b) wood BC, (c, d) rice husk BC, and (e, f) bamboo BC. Magnifications are included in the images, all of which were taken from the same sample orientations.

Preprints (www.preprints.org) | NOT PEER-REVIEWED | Posted: 22 July 2018 doi:10.20944/preprints201807.0403.v1

3.5 Optimising the biochar selection for specific applications

The detailed characterisation of the biochars presented here is the first step in an ongoing project to support local agriculture in Vietnam by optimising the functional capacity of biochars through selection of the most suitable biomass or combination of biomass sources to produce biochars with the desired functional characteristics depending on the intended application. Thus, where the goal is improvement of soil quality, for example via providing a carbon sink or encouraging colonisation by microorganisms the set of desired BC properties needed would be different than those required for applications such as binding of heavy metals or other toxicants or indeed for soil conditioning via enhanced retention of vital nutrients. Table 3 below presents an initial analysis of the BC properties required for the three main applications of interest in this work, and a first mapping of the physical-chemical properties of the three biochars analysed here (wood, risk husk and bamboo) to these requirements. Subsequent work will confirm experimentally that the properties identified in theory as correlating with key functional behaviours, which translate in practice to assessing the ammonium-nitrogen binding and heavy metal binding capacity of the different biochars and correlating these with key physico-chemical properties driving the reactive potential of the biochars.

Table 3: Summary of the BC properties required for different applications and an initial assessment of the suitability of the different BCs match to these properties.

Environmental application	Wood BC	Rice BC	Bamboo BC
Improving soil quality (C sink)			
- High C content	✓	X	✓
- Low Ash content	✓	X	✓
- Alkaline pH	✓	✓	✓
- High surface area	✓	X	✓
- Highly porous structure (habitat for microrganisms and water holding capacity)	✓	X	✓
Binding of heavy metals (remediation)			
- Alkaline pH	✓	✓	✓
- High CEC	X	✓	✓
- High surface area	✓	X	✓
- Alcohol groups / phenols / esters	✓	✓	✓
- Acidic groups (COO^-, CO_3^{2-})	✓	✓	✓
- Other groups (PO_4^{3-})	✓	✓	X
Retention of nutrients (fertilisation)			
- High CEC	X	✓	✓

Preprints (www.preprints.org) | NOT PEER-REVIEWED | Posted: 22 July 2018 doi:10.20944/preprints201807.0403.v1

- High Surface area	✓	✓	✓
- Porous structure	✓	X	✓
- Acidic groups (COO^-, CO_3^{2-})	✓	✓	✓
- Other groups (PO_4^{3-}, Si-O-Si)	✓	✓	X

4. Conclusions

The comparison of three biochars, from different biomass sources widely available in Vietnam (i.e. Acacia wood, rice husk and bamboo), produced using a pyrolysis approach indicated important differences of the physicochemical properties among the biochars produced under identical conditions. The high carbon content and alkaline pH of the three BCs makes them suitable for creating a carbon sink and improving the pH of acidic soils, as well as theoretically providing the capability to reduce mobility of toxic metals by precipitation. The immobility of heavy metals governed by changes pH in soil amended with biochar was reported by precious studies [66-71]. The formation of metal hydr(oxide), carbonate, and phospate precipitates are one of possible mechanisms for the immobility of the metals [66]. Testing of the metal mobility reduction of the biochars is underway and will be reported separately.

CEC and BET surface area are important parameters determining the adsorption capacity of a BC for ion nutrients or heavy metals, so the high CEC values (rice husk BC) and BET surface area values (bamboo BC and wood BC) are useful for soil enrichment and environmental mitigation. The values of CEC relate to cation binding capacity (Ca^{2+}, Mg^2, K^+, Na^+) and functional groups on surface, while BET surface area corresponds to surface morphology, as observed by SEM. The complex morphology with variously sized pores present in bamboo and wood BC not only serves as habitat for microorganisms, but also potentially improves the water holding capacity of soil.

Thus, the detailed characterisation of the biochars is the first step towards optimisation of the selection of biochars for specific applications, as part of an ongoing project to support local agriculture. Indeed, it might be that mixtures of different biomass sources could be developed to fully optimise the functionality of the BCs for a range of agricultural applications.

Acknowledgements

The authors would like to thank the Vietnamese government through the Ministry of Agriculture and Rural Development and the Vietnam International Education Development (VIED) - Ministry

of Education and Training, known as "The priority programme of development and application of biotechnology to agriculture and rural development up to 2020 (Grant Agreement N° 11/2006//QĐ -TTg) for support and funding. Additional support and funding for the project came from EU FP7 Marie Curie Career Integration Grant EcoFriendlyNano (Grant Agreement no. PCIG14-GA-2013-631612). The authors acknowledge excellent technical support from Drs. Anastasios Papadiamantis, Maria Thompson, Lianne Hill, and Paul Stanley of University of Birmingham (UK), Stephen Joseph (University of New South Wales, Australia), Do Duc Khoi (Population, Environment and Development Centre, Vietnam), and Le Xuan Anh (Soils and Fertilizers Research Institute, Vietnam).

References

1. (a) Mukherjee, A.; Zimmerman, A. R., Organic carbon and nutrient release from a range of laboratory-produced biochars and biochar–soil mixtures. *Geoderma* **2013,** *193–194*, 122-130; (b) Paethanom, A.; Yoshikawa, K., Influence of pyrolysis temperature on rice husk char characteristics and its tar adsorption capability. *Energies* **2012,** *5* (12), 4941-4951.
2. Qiu, Y.; Zheng, Z.; Zhou, Z.; Sheng, G. D., Effectiveness and mechanisms of dye adsorption on a straw-based biochar. *Bioresource technology* **2009,** *100* (21), 5348-51.
3. Al-Wabel, M. I.; Al-Omran, A.; El-Naggar, A. H.; Nadeem, M.; Usman, A. R. A., Pyrolysis temperature induced changes in characteristics and chemical composition of biochar produced from conocarpus wastes. *Bioresource Technology* **2013,** *131*, 374-379.
4. Kim, K. H.; Kim, J.-Y.; Cho, T.-S.; Choi, J. W., Influence of pyrolysis temperature on physicochemical properties of biochar obtained from the fast pyrolysis of pitch pine (Pinus rigida). *Bioresource Technology* **2012,** *118*, 158-162.
5. Demirbas, A., Effects of temperature and particle size on bio-char yield from pyrolysis of agricultural residues. *Journal of Analytical and Applied Pyrolysis* **2004,** *72* (2), 243-248.
6. Duku, M. H.; Gu, S.; Hagan, E. B., Biochar production potential in Ghana—a review. *Renewable and Sustainable Energy Reviews* **2011,** *15* (8), 3539-3551.
7. Sohi, S.; Lopez-Capel, E.; Krull, E.; Bol, R., Biochar, climate change and soil: A review to guide future research. *CSIRO Land and Water Science Report* **2009,** *5* (09), 17-31.
8. Schmidt, M. W.; Noack, A. G., Black carbon in soils and sediments: analysis, distribution, implications, and current challenges. *Global biogeochemical cycles* **2000,** *14* (3), 777-793.
9. Zheng, W.; Guo, M.; Chow, T.; Bennett, D. N.; Rajagopalan, N., Sorption properties of greenwaste biochar for two triazine pesticides. *Journal of Hazardous Materials* **2010,** *181* (1–3), 121-126.
10. Neves, E. G.; Petersen, J. B.; Bartone, R. N.; Da Silva, C. A., Historical and socio-cultural origins of Amazonian dark earth. In *Amazonian dark earths*, Springer: 2003; pp 29-50.
11. Masiello, C. A.; Druffel, E. R. M., Black Carbon in Deep-Sea Sediments. *Science* **1998,** *280* (5371), 1911-1913.
12. Major, J.; Rondon, M.; Molina, D.; Riha, S. J.; Lehmann, J., Maize yield and nutrition during 4 years after biochar application to a Colombian savanna oxisol. *Plant and soil* **2010,** *333* (1-2), 117-128.
13. Jones, D. L.; Edwards-Jones, G.; Murphy, D. V., Biochar mediated alterations in herbicide breakdown and leaching in soil. *Soil Biology and Biochemistry* **2011,** *43* (4), 804-813.
14. Sohi, S. P.; Krull, E.; Lopez-Capel, E.; Bol, R., Chapter 2 - A Review of Biochar and Its Use and Function in Soil. In *Advances in Agronomy*, Academic Press: **2010**; Vol. Volume 105, pp 47-82.
15. Liu, Y. Y., M.; Wu, Y.; Wang, H.; Chen, Y.; Wu, W., Reducing CH4 and CO2 emissions from waterlogged paddy soil with biochar. *J Soils Sediments* **2011,** *11*, 930-939.

16. Hale, S. E. A., V.; Martinsen, V.; Mulder, J.; Breedveld, G. D.; Cornelissen, G., The sorption and desorption of phosphate-P, ammonium-N and nitrate-N in cacao shell and corn cob biochars. *Chemosphere* **2013,** *91*, 1612-1619.
17. Huang, M.; Yang, L.; Qin, H.; Jiang, L.; Zou, Y., Fertilizer nitrogen uptake by rice increased by biochar application. *Biology and Fertility of Soils* **2014,** *50* (6), 997-1000.
18. Lehmann, J.; Rondon, M., Bio-char soil management on highly weathered soils in the humid tropics. *Biological approaches to sustainable soil systems. CRC Press, Boca Raton, FL* **2006**, 517-530.
19. Jenkinson, D.; Ayanaba, A., Decomposition of carbon-14 labeled plant material under tropical conditions. *Soil Science Society of America Journal* **1977,** *41* (5), 912-915.
20. Joseph, S.; Lehmann, J., *Biochar for environmental management: science and technology*. London, GB: Earthscan: 2009.
21. Lentz, R.; Ippolito, J., Biochar and manure affect calcareous soil and corn silage nutrient concentrations and uptake. *Journal of environmental quality* **2012,** *41* (4), 1033-1043.
22. Ameloot, N.; De Neve, S.; Jegajeevagan, K.; Yildiz, G.; Buchan, D.; Funkuin, Y. N.; Prins, W.; Bouckaert, L.; Sleutel, S., Short-term CO2 and N2O emissions and microbial properties of biochar amended sandy loam soils. *Soil Biology and Biochemistry* **2013,** *57*, 401-410.
23. (a) Novak, J. M.; Lima, I.; Xing, B.; Gaskin, J. W.; Steiner, C.; Das, K.; Ahmedna, M.; Rehrah, D.; Watts, D. W.; Busscher, W. J., Characterization of designer biochar produced at different temperatures and their effects on a loamy sand. *Ann. Environ. Sci* **2009,** *3* (2); (b) Angın, D., Effect of pyrolysis temperature and heating rate on biochar obtained from pyrolysis of safflower seed press cake. *Bioresource technology* **2013,** *128*, 593-597.
24. Méndez, A.; Tarquis, A. M.; Saa-Requejo, A.; Guerrero, F.; Gascó, G., Influence of pyrolysis temperature on composted sewage sludge biochar priming effect in a loamy soil. *Chemosphere* **2013,** *93* (4), 668-676.
25. Uchimiya, M.; Wartelle, L. H.; Klasson, K. T.; Fortier, C. A.; Lima, I. M., Influence of pyrolysis temperature on biochar property and function as a heavy metal sorbent in soil. *Journal of Agricultural and Food Chemistry* **2011,** *59* (6), 2501-2510.
26. Song, W.; Guo, M., Quality variations of poultry litter biochar generated at different pyrolysis temperatures. *Journal of Analytical and Applied Pyrolysis* **2012,** *94*, 138-145.
27. Mukherjee, A.; Zimmerman, A.; Harris, W., Surface chemistry variations among a series of laboratory-produced biochars. *Geoderma* **2011,** *163* (3), 247-255.
28. Chen, B.; Zhou, D.; Zhu, L., Transitional adsorption and partition of nonpolar and polar aromatic contaminants by biochars of pine needles with different pyrolytic temperatures. *Environmental Science & Technology* **2008,** *42* (14), 5137-5143.
29. Cheng, C.-H.; Lehmann, J.; Engelhard, M. H., Natural oxidation of black carbon in soils: Changes in molecular form and surface charge along a climosequence. *Geochimica et Cosmochimica Acta* **2008,** *72* (6), 1598-1610.
30. Mukome, F. N.; Zhang, X.; Silva, L. C.; Six, J.; Parikh, S. J., Use of chemical and physical characteristics to investigate trends in biochar feedstocks. *Journal of agricultural and food chemistry* **2013,** *61* (9), 2196-2204.
31. Cantrell, K. B.; Hunt, P. G.; Uchimiya, M.; Novak, J. M.; Ro, K. S., Impact of pyrolysis temperature and manure source on physicochemical characteristics of biochar. *Bioresource technology* **2012,** *107*, 419-428.
32. Joseph, S.; Camps-Arbestain, M.; Lin, Y.; Munroe, P.; Chia, C.; Hook, J.; Van Zwieten, L.; Kimber, S.; Cowie, A.; Singh, B., An investigation into the reactions of biochar in soil. *Soil Research* **2010,** *48* (7), 501-515.
33. Gaskin, J.; Steiner, C.; Harris, K.; Das, K.; Bibens, B., Effect of low-temperature pyrolysis conditions on biochar for agricultural use. *Trans. Asabe* **2008,** *51* (6), 2061-2069.
34. Nguyen, B. T.; Lehmann, J., Black carbon decomposition under varying water regimes. *Organic Geochemistry* **2009,** *40* (8), 846-853.
35. Liang, B.; Lehmann, J.; Solomon, D.; Kinyangi, J.; Grossman, J.; O'Neill, B.; Skjemstad, J. O.; Thies, J.; Luizão, F. J.; Petersen, J.; Neves, E. G., Black Carbon Increases Cation Exchange Capacity in Soils. *Soil Science Society of America Journal* **2006,** *70* (5).

36. Cheng, C.-H.; Lehmann, J.; Thies, J. E.; Burton, S. D.; Engelhard, M. H., Oxidation of black carbon by biotic and abiotic processes. *Organic Geochemistry* **2006,** *37* (11), 1477-1488.
37. Yang, F.; Zhao, L.; Gao, B.; Xu, X.; Cao, X., The Interfacial Behavior between Biochar and Soil Minerals and Its Effect on Biochar Stability. *Environmental science & technology* **2016,** *50* (5), 2264-2271.
38. Nasser, R. A.-S.; Aref, I. M., *Fuelwood Characteristics of Six Acacia Species Growing Wild in the Southwest of Saudi Arabia as Affected by Geographical Location*. 2014; Vol. 9.
39. Guo, Y.; Yang, S.; Yu, K.; Zhao, J.; Wang, Z.; Xu, H., The preparation and mechanism studies of rice husk based porous carbon. *Materials Chemistry and Physics* **2002,** *74* (3), 320-323.
40. Hernandez-Mena, L. E.; Pécoraa, A. A.; Beraldob, A. L., Slow pyrolysis of bamboo biomass: Analysis of biochar properties. *CHEMICAL ENGINEERING* **2014,** *37*.
41. Bachmann, H. J.; Bucheli, T. D.; Dieguez-Alonso, A.; Fabbri, D.; Knicker, H.; Schmidt, H.-P.; Ulbricht, A.; Becker, R.; Buscaroli, A.; Buerge, D.; Cross, A.; Dickinson, D.; Enders, A.; Esteves, V. I.; Evangelou, M. W. H.; Fellet, G.; Friedrich, K.; Gasco Guerrero, G.; Glaser, B.; Hanke, U. M.; Hanley, K.; Hilber, I.; Kalderis, D.; Leifeld, J.; Masek, O.; Mumme, J.; Carmona, M. P.; Calvelo Pereira, R.; Rees, F.; Rombolà, A. G.; de la Rosa, J. M.; Sakrabani, R.; Sohi, S.; Soja, G.; Valagussa, M.; Verheijen, F.; Zehetner, F., Toward the Standardization of Biochar Analysis: The COST Action TD1107 Interlaboratory Comparison. *Journal of Agricultural and Food Chemistry* **2016,** *64* (2), 513-527.
42. Rajkovich, S.; Enders, A.; Hanley, K.; Hyland, C.; Zimmerman, A. R.; Lehmann, J., Corn growth and nitrogen nutrition after additions of biochars with varying properties to a temperate soil. *Biology and Fertility of Soils* **2012,** *48* (3), 271-284.
43. Brunauer, S.; Emmett, P. H.; Teller, E., Adsorption of gases in multimolecular layers. *J. Am. Chem. Soc* **1938,** *60* (2), 309-319.
44. Bagreev, A.; Bandosz, T. J.; Locke, D. C., Pore structure and surface chemistry of adsorbents obtained by pyrolysis of sewage sludge-derived fertilizer. *Carbon* **2001,** *39* (13), 1971-1979.
45. Gundale, M. J.; DeLuca, T. H., Temperature and source material influence ecological attributes of ponderosa pine and Douglas-fir charcoal. *Forest Ecology and Management* **2006,** *231* (1–3), 86-93.
46. Yuan, J.-H.; Xu, R.-K.; Zhang, H., The forms of alkalis in the biochar produced from crop residues at different temperatures. *Bioresource technology* **2011,** *102* (3), 3488-3497.
47. Lee, Y.; Park, J.; Ryu, C.; Gang, K. S.; Yang, W.; Park, Y.-K.; Jung, J.; Hyun, S., Comparison of biochar properties from biomass residues produced by slow pyrolysis at 500 C. *Bioresource technology* **2013,** *148*, 196-201.
48. Shen, Y.; Zhao, P.; Shao, Q., Porous silica and carbon derived materials from rice husk pyrolysis char. *Microporous and Mesoporous Materials* **2014,** *188*, 46-76.
49. Sharma, R. K.; Wooten, J. B.; Baliga, V. L.; Lin, X.; Geoffrey Chan, W.; Hajaligol, M. R., Characterization of chars from pyrolysis of lignin. *Fuel* **2004,** *83* (11–12), 1469-1482.
50. (a) Yargicoglu, E. N.; Sadasivam, B. Y.; Reddy, K. R.; Spokas, K., Physical and chemical characterization of waste wood derived biochars. *Waste Management* **2015,** *36*, 256-268; (b) Enders, A.; Hanley, K.; Whitman, T.; Joseph, S.; Lehmann, J., Characterization of biochars to evaluate recalcitrance and agronomic performance. *Bioresource technology* **2012,** *114*, 644-653.
51. Budai, A.; Wang, L.; Gronli, M.; Strand, L. T.; Antal Jr, M. J.; Abiven, S.; Dieguez-Alonso, A.; Anca-Couce, A.; Rasse, D. P., Surface properties and chemical composition of corncob and Miscanthus biochars: effects of production temperature and method. *Journal of agricultural and food chemistry* **2014,** *62* (17), 3791-3799.
52. Essington, M. E., *Soil and water chemistry: An integrative approach*. CRC press: 2015.
53. Harvey, O. R.; Herbert, B. E.; Rhue, R. D.; Kuo, L.-J., Metal interactions at the biochar-water interface: energetics and structure-sorption relationships elucidated by flow adsorption microcalorimetry. *Environmental science & technology* **2011,** *45* (13), 5550-5556.
54. Stuart, B. H., Spectral analysis. *Infrared spectroscopy: fundamentals and applications* **2004**, 45-70.
55. Fang, Q.; Chen, B.; Lin, Y.; Guan, Y., Aromatic and Hydrophobic Surfaces of Wood-derived Biochar Enhance Perchlorate Adsorption via Hydrogen Bonding to Oxygen-containing Organic Groups. *Environmental Science & Technology* **2014,** *48* (1), 279-288.
56. Keiluweit, M.; Nico, P. S.; Johnson, M. G.; Kleber, M., Dynamic molecular structure of plant biomass-derived black carbon (biochar). *Environmental science & technology* **2010,** *44* (4), 1247-1253.

662 57. Fu, P.; Yi, W.; Bai, X.; Li, Z.; Hu, S.; Xiang, J., Effect of temperature on gas composition and char
663 structural features of pyrolyzed agricultural residues. *Bioresource technology* **2011,** *102* (17), 8211-8219.
664 58. Rouquerol, J.; Avnir, D.; Fairbridge, C.; Everett, D.; Haynes, J.; Pernicone, N.; Ramsay, J.; Sing, K.;
665 Unger, K., Recommendations for the characterization of porous solids (Technical Report). *Pure and Applied*
666 *Chemistry* **1994,** *66* (8), 1739-1758.
667 59. Cetin, E.; Moghtaderi, B.; Gupta, R.; Wall, T., Influence of pyrolysis conditions on the structure and
668 gasification reactivity of biomass chars. *Fuel* **2004,** *83* (16), 2139-2150.
669 60. Sharma, R. K.; Wooten, J. B.; Baliga, V. L.; Martoglio-Smith, P. A.; Hajaligol, M. R., Characterization
670 of char from the pyrolysis of tobacco. *Journal of agricultural and food chemistry* **2002,** *50* (4), 771-783.
671 61. Septien, S.; Valin, S.; Peyrot, M.; Spindler, B.; Salvador, S., Influence of steam on gasification of
672 millimetric wood particles in a drop tube reactor: Experiments and modelling. *Fuel* **2013,** *103*, 1080-1089.
673 62. Liu, Z.; Zhang, F.-S.; Wu, J., Characterization and application of chars produced from pinewood
674 pyrolysis and hydrothermal treatment. *Fuel* **2010,** *89* (2), 510-514.
675 63. Septien, S.; Valin, S.; Dupont, C.; Peyrot, M.; Salvador, S., Effect of particle size and temperature on
676 woody biomass fast pyrolysis at high temperature (1000–1400 C). *Fuel* **2012,** *97*, 202-210.
677 64. Thies, J. E.; Rillig, M. C., Characteristics of biochar: biological properties. *Biochar for environmental*
678 *management: Science and technology* **2009**, 85-105.
679 65. (a) Guerrero, M.; Ruiz, M. P.; Alzueta, M. U.; Bilbao, R.; Millera, A., Pyrolysis of eucalyptus at
680 different heating rates: studies of char characterization and oxidative reactivity. *Journal of Analytical and*
681 *Applied Pyrolysis* **2005,** *74* (1–2), 307-314; (b) Onay, O., Influence of pyrolysis temperature and heating rate
682 on the production of bio-oil and char from safflower seed by pyrolysis, using a well-swept fixed-bed
683 reactor. *Fuel Processing Technology* **2007,** *88* (5), 523-531.
684 66. Park, J. H.; Choppala, G. K.; Bolan, N. S.; Chung, J. W.; Chuasavathi, T., Biochar reduces the
685 bioavailability and phytotoxicity of heavy metals. *Plant and soil* **2011,** *348* (1-2), 439.
686 67. Ehsan, M.; Barakat, M.; Husein, D. Z.; Ismail, S., Immobilization of Ni and Cd in soil by biochar
687 derived from unfertilized dates. *Water, Air, & Soil Pollution* **2014,** *225* (11), 2123.
688 68. Herath, I.; Kumarathilaka, P.; Navaratne, A.; Rajakaruna, N.; Vithanage, M., Immobilization and
689 phytotoxicity reduction of heavy metals in serpentine soil using biochar. *Journal of soils and sediments*
690 **2015,** *15* (1), 126-138.
691 69. Houben, D.; Evrard, L.; Sonnet, P., Mobility, bioavailability and pH-dependent leaching of cadmium,
692 zinc and lead in a contaminated soil amended with biochar. *Chemosphere* **2013,** *92* (11), 1450-1457.
693 70. Jiang, J.; Xu, R.-k.; Jiang, T.-y.; Li, Z., Immobilization of Cu (II), Pb (II) and Cd (II) by the addition of
694 rice straw derived biochar to a simulated polluted Ultisol. *Journal of hazardous materials* **2012,** *229*, 145-
695 150.
696 71. Ahmad, M.; Lee, S. S.; Yang, J. E.; Ro, H.-M.; Lee, Y. H.; Ok, Y. S., Effects of soil dilution and
697 amendments (mussel shell, cow bone, and biochar) on Pb availability and phytotoxicity in military shooting
698 range soil. *Ecotoxicology and environmental safety* **2012,** *79*, 225-231.

Preprints (www.preprints.org) | NOT PEER-REVIEWED | Posted: 22 July 2018 doi:10.20944/preprints201807.0403.v1

699

700 ToC figure

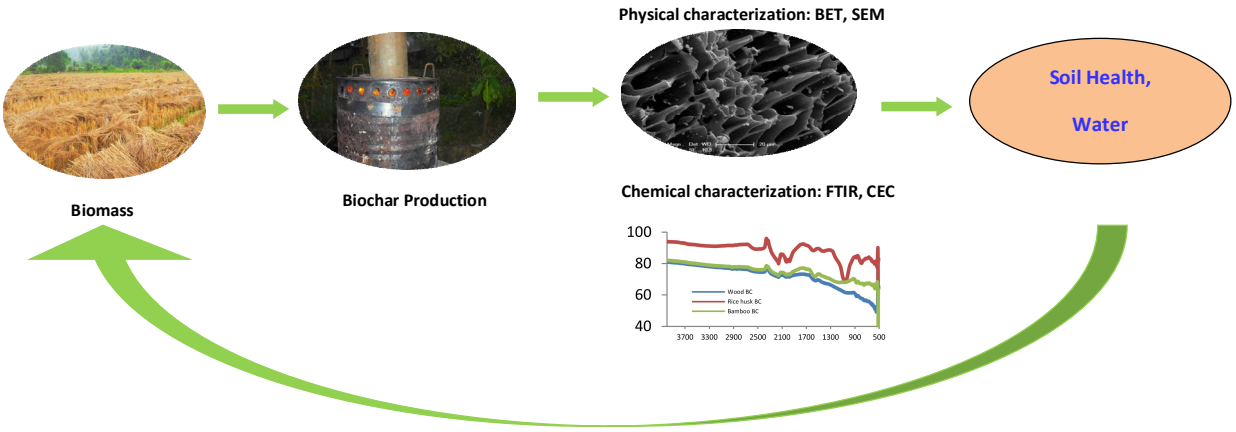

701